

# Radiative Neutron Capture on Lithium-7

Gautam Rupak\*

*Department of Physics & Astronomy and High Performance Computing Collaboratory,  
Mississippi State University, Mississippi State, MS 39762, U.S.A.*

Renato Higa†

*Kernfysisch Versneller Instituut, Theory Group,  
University of Groningen, 9747AA Groningen, The Netherlands*

## Abstract

The radiative neutron capture on lithium-7 is calculated model independently using a low energy halo effective field theory. The cross section is expressed in terms of scattering parameters directly related to the  $S$ -matrix element. The cross section depends on the poorly known  $p$ -wave effective range parameter  $r_1$ . This constitutes the leading order uncertainty in traditional model calculations. It is explicitly demonstrated by comparing with potential model calculations. A single parameter fit describes the low energy data extremely well and yields  $r_1 \approx -1.47 \text{ fm}^{-1}$ .

Keywords: radiative capture, halo nuclei, effective field theory

arXiv:1101.0207v1 [nucl-th] 31 Dec 2010

---

\* grupak@u.washington.edu

† R.Higa@rug.nl

## I. INTRODUCTION

Low energy nuclear reactions play a crucial role in Big Bang Nucleosynthesis (BBN), stellar burning and element synthesis at supernova sites [1–3]. Besides placing constraints on our understanding of element formation, these low energy reactions play an important role in testing astrophysical models and physics beyond the Standard Model of particle physics. Often the key nuclear reactions occur at energies that are not directly accessible in terrestrial laboratories. Radiative proton capture on beryllium  ${}^7\text{Be}(p,\gamma){}^8\text{B}$  is one of them —it is important for boron-8 production in the sun, whose weak decay results in the high energy neutrinos that are detected at terrestrial laboratories looking for physics beyond the Standard Model. The relevant solar energy, the Gamow peak, for this reaction is around 20 keV [4]. This necessitates extrapolation to solar energies of known experimental capture cross sections from above around 100 keV. Theoretical input becomes necessary for this extrapolation. Effective field theory (EFT) is an ideal formalism for this as it provides a model-independent calculation with reliable error estimates.

In an EFT, one identifies the relevant low energy degrees of freedom and constructs the most general interactions allowed by symmetry without modeling the short distance physics. The interactions are organized in a low momentum expansion. At a given order in the expansion, a finite number of interactions has to be considered and an *a priori* estimate of the theoretical error can be made. Establishing theoretical errors is crucial due to astrophysical demands [1, 2, 4]. A systematic expansion of interactions is important because many processes involve external currents, and any prescription used in phenomenological models involve some uncertainty. As an example, the cross section for  $n(p,\gamma)d$  at BBN energies was calculated within EFT to an accuracy of about 1% [5]. Systematic treatment of two-body currents was necessary to achieve this level of precision, and it addressed a critical need [1] for nuclear theory input in astrophysics.

While applications of EFT to systems with  $A \lesssim 4$  nucleons is well developed, for  $A \gtrsim 5$  it is still in its infancy. However, some loosely bound systems, like halo nuclei open new possibilities. The small separation energy of the valence nucleons in halo nuclei provides a small expansion parameter for constructing a halo EFT [6]. The  ${}^8\text{B}$  nucleus with a proton weakly bound to the  ${}^7\text{Be}$  core by 0.1375 MeV is a halo system. Current extrapolation of the  ${}^7\text{Be}(p,\gamma){}^8\text{B}$  cross section to solar energies introduce errors in the 5 – 20% range [4, 7, 8]. A model-independent EFT calculation would be very useful to estimate the errors in the extrapolation. In addition, this would be an important step in developing EFT techniques for weakly-bound nuclei as has been accomplished in the few nucleon systems. Experiments such as those planned at the future FRIB [9] would explore exotic nuclei near the drip lines where halo systems abound. Structures and reactions with halo EFT can serve as benchmark for phenomenological models of nuclei near the drip lines.

In this paper we consider the low energy reaction  ${}^7\text{Li}(n,\gamma){}^8\text{Li}$ , which is a isospin mirror to  ${}^7\text{Be}(p,\gamma){}^8\text{B}$ . The  $n$ - ${}^7\text{Li}$  system allows formulating the EFT for the nuclear interactions without the added complication of the Coulomb force. Traditionally  ${}^7\text{Li}(n,\gamma){}^8\text{Li}$  has been calculated in a single-particle approximation as a  ${}^7\text{Li}$  core plus a valence neutron interacting via a Woods-Saxon potential [10]. This approximation breaks down at higher energies when the internal structure of the  ${}^7\text{Li}$  core is probed, for example, near the threshold for  ${}^7\text{Li}(\gamma,{}^3\text{He})\alpha$  which is about 0.5 MeV above the binding energy  $B \approx 2.03$  MeV of the  ${}^8\text{Li}$  core. We treat the  ${}^7\text{Li}$  nucleus as point-like since we work at very low energies. Once the nuclear piece is calculated in EFT for the  $n$ - ${}^7\text{Li}$  system the Coulomb interaction in  $p$ - ${}^7\text{Be}$  can be incorporated systematically as have been done for proton fusion in EFT [11]. The reaction  ${}^7\text{Li}(n,\gamma){}^8\text{Li}$ , besides being a check on the mirror  ${}^7\text{Be}(p,\gamma){}^8\text{B}$  reaction, is important in inhomogeneous BBN. It impacts the production of carbon-oxygen-nitrogen in the early universe, and constrains astrophysical models [12]. We calculate the

${}^7\text{Li}(n, \gamma){}^8\text{Li}$  reaction analytically and express the result in terms of parameters directly related to observables, thus quantifying the dominant theoretical uncertainty in the single particle approximation.

## II. INTERACTION

The relevant low energy nuclear degrees of freedom, here, are the point-like neutron,  ${}^7\text{Li}$  and  ${}^8\text{Li}$  with spin-parity  $\frac{1}{2}^+$ ,  $\frac{3}{2}^-$  and  $2^+$  respectively. At low energies the relevant partial waves in the incoming neutron-lithium state are  $s$ -waves:  ${}^3S_1$ ,  ${}^5S_2$  in the spectroscopic notation  ${}^{2S+1}L_J$ . The ground state is a  $2^+$  state that is primarily the symmetric combination of the possible  $p$ -wave states  ${}^3P_2$  and  ${}^5P_2$  [13]. Conservation of parity implies that the reaction  ${}^7\text{Li}(n, \gamma){}^8\text{Li}$  proceeds through the electric dipole transition E1 at lowest order.

It is known that the non-relativistic amplitude in the  $l$ -th partial wave has the general form

$$i\mathcal{A}_l(p) = \frac{2\pi}{\mu} \frac{ip^{2l}}{p^{2l+1} \cot \delta_l - ip^{2l+1}}, \quad (1)$$

where  $\mu$  is the reduced mass of the  $n$ - ${}^7\text{Li}$  system with masses  $M_N$  and  $M_C$ , respectively, and  $\delta_l$  is the partial wave phase shift. The term  $p^{2l+1} \cot \delta_l = -1/a_l + r_l p^2/2 + \dots$  has an analytic effective range expansion (ERE) for short range interactions. Scattering and bound state information in EFT are incorporated by matching the EFT couplings to the ERE parameters in the low energy expansion.

For the initial  $s$ -wave states, at sufficiently low momentum  $i\mathcal{A}_0 \approx -i\frac{2\pi}{\mu}a_0$ , and one keeps only the first term in the ERE, corresponding to a single perturbative insertion of the leading EFT interaction. However, to describe shallow bound or virtual states that correspond to large scattering length  $a_0 \gg r_0$  one has to expand around the  $1/a_0$  pole term and write

$$i\mathcal{A}_0 \approx i\frac{2\pi}{\mu} \frac{1}{-\frac{1}{a_0} - ip} \left[ 1 - \frac{r_0 p^2}{2(-\frac{1}{a_0} - ip)} + \dots \right]. \quad (2)$$

This requires a non-perturbative resummation of a single interaction in EFT at leading order. Such a resummation extends the validity of the EFT to include the shallow state at momenta  $p \sim 1/a_0$ . In the  $n$ - ${}^7\text{Li}$  system, the scattering length is  $a_0^{(2)} = -3.63 \pm 0.05$  fm ( $a_0^{(1)} = 0.87 \pm 0.07$  fm) in the  ${}^5S_2$  ( ${}^3S_1$ ) spin-channel [14]. This corresponds to neutron momentum around 54 (227) MeV, or center of mass (CM) energy 2 (31) MeV. We are interested at the extremely low solar energies with momenta  $p \ll 54$  MeV. Thus in EFT a single perturbative interaction in each of the  ${}^5S_2$  and  ${}^3S_1$  channels is required. The interaction can be resummed in the  ${}^5S_2$  channel if one wants to compare with data at CM energies  $\sim 1$  MeV.

The leading order interactions for  $s$ -wave contain no derivatives. The spin- $\frac{1}{2}$  neutron and spin- $\frac{3}{2}$   ${}^7\text{Li}$  nucleus can be combined into the  ${}^3S_1$  and  ${}^5S_2$  states using the Clebsch-Gordan coefficient matrices  $F_i$ ,  $Q_{ij}$  as  $N^T F_i C$  and  $N^T Q_{ij} C$  respectively. The vector index in  $F_i$  relates to the three magnetic quantum numbers in the spin  $S = 1$  channel. The symmetric, traceless matrices  $Q_{ij}$  relate to the five magnetic quantum numbers in the spin  $S = 2$  channel. We write the  $s$ -wave interaction Lagrangian as

$$\mathcal{L}^{(s)} = g^{(1)}(N F_i C)^\dagger (N F_i C) + g^{(2)}(N Q_{ij} C)^\dagger (N Q_{ij} C) + \dots, \quad (3)$$

where a single momentum-independent interaction in each of the  $^3S_1$  and  $^5S_2$  channels was kept. The “...” represents higher derivative terms that are suppressed at low energy. The  $2 \times 4$  Clebsch-Gordan matrices are given as

$$F_i = -\frac{i\sqrt{3}}{2}\sigma_2 S_i, \quad Q_{ij} = -\frac{i}{\sqrt{8}}\sigma_2[\sigma_i S_i + \sigma_j S_j], \quad (4)$$

$$S_1 = \frac{1}{\sqrt{6}} \begin{pmatrix} -\sqrt{3} & 0 & 1 & 0 \\ 0 & -1 & 0 & \sqrt{3} \end{pmatrix}, \quad S_2 = -\frac{i}{\sqrt{6}} \begin{pmatrix} \sqrt{3} & 0 & 1 & 0 \\ 0 & 1 & 0 & \sqrt{3} \end{pmatrix}, \quad S_3 = \frac{2}{\sqrt{6}} \begin{pmatrix} 0 & 1 & 0 & 0 \\ 0 & 0 & 1 & 0 \end{pmatrix}.$$

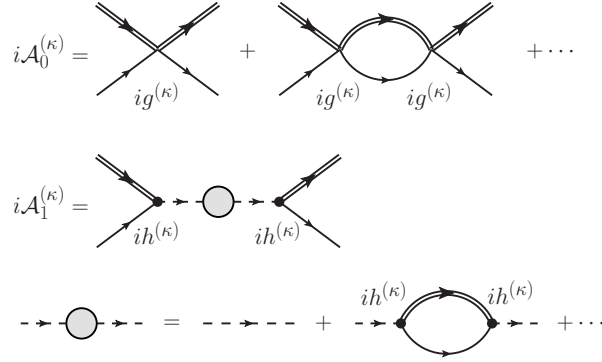


FIG. 1.  $\mathcal{A}_0^{(\kappa)}$  is the  $^3S_1$ ,  $^5S_2$  scattering amplitude.  $\mathcal{A}_1^{(\kappa)}$  is the  $^3P_2$ ,  $^5P_2$  scattering amplitude. Double line is the  $^7\text{Li}$  propagator, single line the neutron propagator, dashed line the bare dimer propagator.

The interaction in Eq. (3) produces a  $s$ -wave amplitude shown in Fig. 1. It becomes a geometric series that is summed to give

$$i\mathcal{A}_{EFT}^{(\kappa)}(p) = \frac{ig^{(\kappa)}}{1 - ig^{(\kappa)}L(p)}, \quad (5)$$

$$L(p) = -i2\mu \left(\frac{\lambda}{2}\right)^{4-D} \int \frac{d^{D-1}\mathbf{q}}{(2\pi)^{D-1}} \frac{1}{q^2 - p^2 - i0^+} = -\frac{i\mu}{2\pi}(\lambda + ip),$$

where  $g^{(\kappa)}$  corresponds to  $g^{(1)}$ ,  $g^{(2)}$  in the respective spin channels and  $\lambda$  is the renormalization scale. The loop integral  $L(p)$  is evaluated in the power divergence subtraction scheme [15] where divergences in both  $D = 4$  and lower space-time dimensions are subtracted. Matching Eqs. (2) and (5) fixes the EFT couplings as  $g^{(\kappa)}(\lambda) = (2\pi)/[\mu(\lambda - 1/a_0^{(\kappa)})]$ . Introduction of the renormalization scale  $\lambda$  allows for a systematic expansion of the different terms even though the final amplitude is independent of  $\lambda$  [16]. In Ref. [17], initial state interactions using ERE was also considered.

The  $^8\text{Li}$  nucleus in the final state of the reaction  $^7\text{Li}(n, \gamma)^8\text{Li}$  is in  $p$ -wave. We will treat it as a shallow bound state similar to its isospin mirror  $^8\text{B}$  nucleus. The EFT for a shallow  $p$ -wave bound state was formulated in Ref. [6] where it was shown that, unlike  $s$ -wave, it requires not one but two non-perturbative EFT interactions. The consistent renormalization of loops is easily accomplished in the dimer formalism where four-fermion interactions are rewritten in terms of a spin-2 dimer and neutron-core interactions. The interactions in the  $^3P_2$  and  $^5P_2$  state can be constructed by combining the matrices  $F_i$ ,  $Q_{ij}$  and the Galilean invariant velocity difference vector  $(\mathbf{v}_C - \mathbf{v}_N)_k$

into a  $p$ -wave state with total  $J = 2$ . We write the  $p$ -wave interaction Lagrangian as

$$\begin{aligned} \mathcal{L}^{(p)} = & \phi_{ij}^\dagger \left[ \Delta^{(1)} + \left( i\partial_0 + \frac{\nabla^2}{2M} \right) \right] \phi_{ij} + h^{(1)} \sqrt{3} \left[ \phi_{ij}^\dagger N F_x \left( \frac{\vec{\nabla}}{M_C} - \frac{\vec{\nabla}}{M_N} \right)_y C + h.c. \right] R_{ijxy} \\ & + \pi_{ij}^\dagger \left[ \Delta^{(2)} + \left( i\partial_0 + \frac{\nabla^2}{2M} \right) \right] \pi_{ij} + \frac{h^{(2)}}{\sqrt{2}} \left[ \pi_{ij}^\dagger N Q_{xy} \left( \frac{\vec{\nabla}}{M_C} - \frac{\vec{\nabla}}{M_N} \right)_z C + h.c. \right] T_{xyzij}, \end{aligned} \quad (6)$$

where  $\phi_{ij}$  ( $\pi_{ij}$ ) is the dimer in the  ${}^3P_2$  ( ${}^5P_2$ ) channel, and

$$R_{ijxy} = \frac{1}{2} [\delta_{ix}\delta_{jy} + \delta_{iy}\delta_{jx} - \frac{2}{3}\delta_{ij}\delta_{xy}], \quad T_{xyzij} = \frac{1}{2} [\varepsilon_{xzi}\delta_{yj} + \varepsilon_{xzt}\delta_{yt} + \varepsilon_{yzi}\delta_{xt} + \varepsilon_{yzt}\delta_{xt}]. \quad (7)$$

The interactions in  $\mathcal{L}^{(p)}$  are equivalent to the ones with only neutron-core short range interactions without a dimer field. In terms of Feynman diagrams, the four-fermion neutron-core interaction is replaced in the dimer formulation by a dimer exchange, Fig. 1. The non-perturbative iteration of the leading operators is accomplished by “dressing” the dimer propagator with nucleon-core loops. For a given spin-channel  $\kappa = 1$  ( ${}^3P_2$ ),  $2$  ( ${}^5P_2$ ) the dressed dimer propagator, which is proportional to the elastic amplitude, reads

$$\begin{aligned} iD^{(\kappa)}(p_0, \mathbf{p}) R_{ijmn} &= \frac{iR_{ijmn}}{\Delta^{(\kappa)} - \frac{1}{2\mu}\zeta^2 + \frac{2h^{(\kappa)2}}{\mu}f(p_0, \mathbf{p})}, \\ f(p_0, \mathbf{p}) &= \frac{1}{4\pi} \left( \zeta^3 - \frac{3}{2}\zeta^2\lambda + \frac{\pi}{2}\lambda^3 \right), \end{aligned} \quad (8)$$

where  $\zeta = \sqrt{-2\mu p_0 + \mu p^2/M - i0^+}$ ,  $M = M_N + M_C$ . Matching the EFT amplitudes to the  $p$ -wave ERE expansion determines the coupling pair  $(\Delta^{(\kappa)}, h^{(\kappa)})$ . Again, only the first two ERE parameters are kept in the low energy expansion since EFT requires two operators at leading order.

### III. RADIATIVE CAPTURE

The leading order capture cross section can be calculated via minimally coupling the photon by gauging the  ${}^7\text{Li}$  core momentum  $\mathbf{p} \rightarrow \mathbf{p} + Z_C e \mathbf{A}$ , where  $Z_C = 3$  is the  ${}^7\text{Li}$  core charge. The E1 contribution to the cross section comes from the diagrams in Fig. 2. The CM kinematics are defined as:  $\mathbf{p}$  the core momentum,  $\mathbf{k}$  the photon momentum and  $\hat{\mathbf{k}} \cdot \hat{\mathbf{p}} = \cos\theta$ . Formally we take  $p \sim \gamma$  as the small scale where  $\gamma = \sqrt{2\mu B} \approx 57.8$  MeV is the  ${}^8\text{Li}$  binding momentum. Then at leading order the Mandelstam variable  $s \approx (M_N + M_C)^2 = M^2$  and  $|\mathbf{k}| = k_0 \approx (p^2 + \gamma^2)/(2\mu)$ . We get for the CM differential cross section

$$\frac{d\sigma}{d\phi d\cos\theta} = \frac{1}{64\pi^2 s} \frac{|\mathbf{k}|}{|\mathbf{p}|} |\mathcal{M}|^2 \approx \frac{1}{64\pi^2 M^2} \frac{p^2 + \gamma^2}{2\mu p} |\mathcal{M}|^2. \quad (9)$$

The capture from the initial state  ${}^5S_2$  to the  ${}^5P_2$  final state (spin channel 2) dominates due to the larger initial state scattering length  $a_0^{(2)} > a_0^{(1)}$ . The divergence in diagram (b) is canceled by (d).

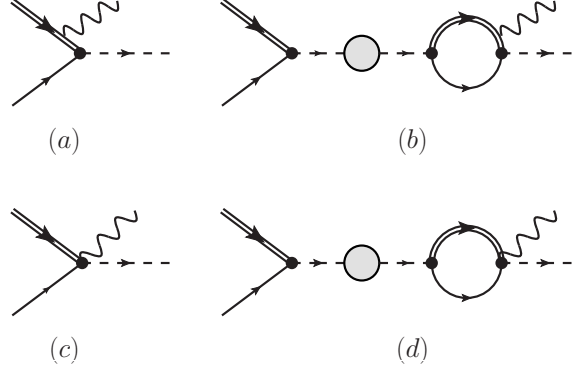


FIG. 2. Capture reactions  ${}^7\text{Li}(n, \gamma){}^8\text{Li}$ . Wavy lines represent photons.

Summing over all polarizations and spins we get

$$|\mathcal{M}({}^5P_2)|^2 = \frac{5|Z_\pi| \left[ 8\pi Z_C h^{(2)} \right]^2 \alpha M M_n}{\pi M_c} \left[ (1+X)(1+X^*) - \frac{p^2 \sin^2 \theta}{p^2 + \gamma^2} \left( \frac{2\gamma^2}{p^2 + \gamma^2} + X + X^* \right) \right], \quad (10)$$

$$X = \frac{i}{-1/a_0^{(2)} - ip} \left( p - i \frac{2\gamma^3 - ip^3}{3(p^2 + \gamma^2)} \right),$$

with the dimer polarization sum  $\sum \epsilon_{ij} \epsilon_{xy}^* = R_{ijxy}$  [18] and the wave function renormalization  $h^{(2)2} |Z_\pi| = 2\pi / |3\gamma + r_1^{(2)}|$ , where  $r_1^{(2)}$  is the effective range in the  ${}^5P_2$  scattering amplitude.  $Z_\pi$  is defined as the residue at the pole in the dressed dimer propagator  $D_\pi(p_0, \mathbf{p})$  [19]. The capture from the  ${}^3S_1$  state to the  ${}^3P_2$  state has the same exact expression as Eq. (10) except that  $a_0^{(2)}$  and  $r_1^{(2)}$  are replaced by the corresponding parameters in the spin channel 1. The differential cross section averaged over initial spin states is

$$\frac{d\sigma}{d\cos\theta} = \frac{1}{32\pi M^2} \frac{p^2 + \gamma^2}{2\mu p} \frac{1}{8} \frac{|\mathcal{M}({}^5P_2)|^2 + |\mathcal{M}({}^3P_2)|^2}{2}, \quad (11)$$

taking the  ${}^8\text{Li}$  nucleus to be a symmetric combination  $(|{}^3P_2\rangle + |{}^5P_2\rangle) / \sqrt{2}$  of final states. The total cross section  $\sigma(p)$  is calculated with a straightforward integration over the angle  $\theta$ .

The parameters in  $\sigma(p)$  can be determined from elastic  $n$ - ${}^7\text{Li}$  scattering data and  ${}^8\text{Li}$  binding energy. However, the  $p$ -wave effective range  $r_1^{(\kappa)}$  is not known accurately. This is the main theoretical uncertainty at this order. Changing the effective range  $r_1^{(\kappa)}$  modifies the wave function renormalization factor and moves the cross section up or down by a constant factor. In traditional potential model calculations, the parameters are determined by reproducing the  ${}^8\text{Li}$  binding energy. However, this does not constrain the effective range and other parameters of the ERE. For example, in a Woods-Saxon potential  $V(r) = -v_0 [1 + \exp(\frac{r-R_c}{a_c})]^{-1}$  different choices for the depth  $v_0$ , range  $R_c$ , diffusiveness  $a_c$  can be made to reproduce the known  ${}^8\text{Li}$  binding energy. This however produces different effective ranges, and constitutes an irreducible source of error in the theoretical calculations.

Comparing the contributions to the capture cross section from the two spin channels analyti-

cally, we get

$$\frac{\sigma(^5P_2)}{\sigma(^5P_2) + \sigma(^3P_2)} \Big|_{p=0} = \frac{(3 - 2a_0^{(2)}\gamma)^2}{(3 - 2a_0^{(2)}\gamma)^2 + (3 - 2a_0^{(1)}\gamma)^2} \approx 0.81, \quad (12)$$

using the same effective range  $r_1$  in both spin channels. This ratio is close to the experimentally observed ratio [20]. From Eqs. (10), (11) one can see that the total cross section at low energy is not independently sensitive to  $r_1^{(2)}$  and  $r_1^{(1)}$ . This is confirmed by our fit to data.

In Fig. 3, we compare potential model calculations using Tombrello’s [10], and Davids-Typel’s [7] parameters to EFT curves. At low energy the potential model results can be reproduced in EFT with a small variation in the effective range  $-0.46 \text{ fm}^{-1} \leq r_1 \leq -0.3 \text{ fm}^{-1}$ . At higher energies they differ since potential models include ERE parameters beyond the scattering length and effective range. A fit to data from Ref. [21] in the energy range  $E_n \sim 2 - 700 \text{ eV}$  gives an effective range  $r_1 = -1.83 \text{ fm}^{-1}$  with only the spin channel 2 contribution and  $r_1 = -1.47 \text{ fm}^{-1}$  with both spin channels 1 and 2. Both the  $r_1$  values are compatible with the Wigner bound [22] which, for a nucleon-core interaction shorter than 3 fm restricts  $r_1$  to be smaller than around  $-1 \text{ fm}^{-1}$ . Following Ref. [21], their data and the theory curves in the right panel in Fig. 3 were divided by the known experimental branching ratio 0.89 to the ground state and compared to a few other available data [23–25]. The  $r_1$  was fitted to the unscaled data for transition to the ground state as appropriate. It is clear that the theory error in the low energy extrapolation comes from the uncertainty in the effective range at leading order.

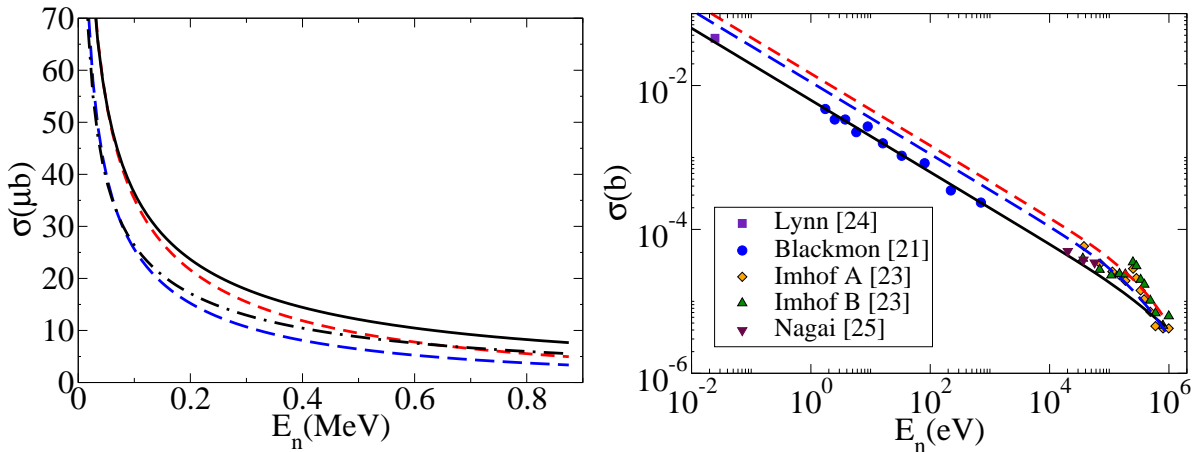


FIG. 3. Potential model curves: (blue) long-dashed curve from Davids-Typel [7], (red) dashed curve from Tombrello [10]. Left panel: (black) solid curve EFT with  $r_1 = -0.46 \text{ fm}^{-1}$ , (black) dot-dashed curve EFT with  $r_1 = -0.3 \text{ fm}^{-1}$ . Right panel: (black) solid curve EFT with  $r_1$  fitted to data.

#### IV. CONCLUSIONS

We considered radiative capture reactions for halo nuclei. The low energy  $^7\text{Li}(n, \gamma)^8\text{Li}$  cross section was calculated at leading order using EFT. In the single particle approximation, the cross section was derived in terms of scattering parameters that are directly related to  $S$ -matrix elements.

Using a model-independent formalism we demonstrated and quantified the theoretical uncertainty associated with phenomenological potentials in the single particle approximation. The leading order result depends on the  $p$ -wave effective range parameter  $r_1$  that is poorly known. Without detailed knowledge about this parameter, model calculations deviate from data at low energy. We extract the effective range  $r_1$  by fitting our analytic form to data.

At higher order in the EFT expansion, the cross section would get corrections from two sources: higher order initial and final state interactions, and two-body currents. The initial and final state interactions can be related to the ERE. At the very low energy, it is the final state interactions, which modify the wave function renormalization constants, that are important. At next-to-next-to-leading order the shape parameter associated with  $p$ -wave interaction contribute [6, 26]. In addition, at higher order two-body currents such as  $E_i(NF_jC)^\dagger[NF_x(\vec{\nabla}/M_C - \overleftarrow{\nabla}/M_N)_yC]R_{ijxy}$ , where  $E_i$  is the electric field, contribute. These operators are not constrained by elastic scattering. A higher order EFT calculation would reduce theoretical errors though at the expense of additional parameters. This is not necessarily a drawback as what we gain is a model-independent understanding of the sources of higher order contributions, and a more detailed knowledge about the kind of experimental input that is required to better constrain the low energy theory.

Coulomb interactions in  $p + {}^7\text{Be}$  scattering and  ${}^7\text{Be}(p, \gamma){}^8\text{B}$  reaction is being considered where the current formulation plays a crucial role [26]. The power counting of electromagnetic currents beyond leading order is being considered as well.

## ACKNOWLEDGMENTS

The authors thank P. Bedaque, C. Bertulani, B. Davids, C. Johnson, A. Mukhamedzhanov, S. Typel for valuable discussions. Authors are extremely grateful to S. Typel for providing the potential model numbers. Authors thank ECT\* and INT, and R.H. thanks MSU for hospitality where part of this research was performed. The work of G.R. is partially supported by the HPCC center at MSU and the U.S. NSF grant PHY-0969378. The work of R.H. was partially supported by the Dutch Stichting voor Fundamenteel Onderzoek der Materie under programme 104 and by the BMBF under contract number 06BN411.

- 
- [1] S. Burles, K. M. Nollett, J. N. Truran, and M. S. Turner, Phys. Rev. Lett., **82**, 4176 (1999).
  - [2] C. Rolfs and W. Rodney, *Cauldrons in the Cosmos* (University Of Chicago Press, London, 1988).
  - [3] S. W. Barwick *et al.*, arXiv:astro-ph/0412544.
  - [4] E. G. Adelberger *et al.*, Rev. Mod. Phys., **70**, 1265 (1998).
  - [5] G. Rupak, Nucl. Phys., **A678**, 405 (2000).
  - [6] C. A. Bertulani, H. W. Hammer, and U. Van Kolck, Nucl. Phys., **A712**, 37 (2002); P. F. Bedaque, H. W. Hammer, and U. van Kolck, Phys. Lett., **B569**, 159 (2003).
  - [7] B. Davids and S. Typel, Phys. Rev. C, **68**, 045802 (2003).
  - [8] P. Descouvemont, Phys. Rev. C, **70**, 065802 (2004).
  - [9] The Facility for Rare Isotope Beams (FRIB) will be a new National User Facility at the Michigan State University, <http://frib.msu.edu/>.
  - [10] T. Tombrello, Nuclear Physics, **71**, 459 (1965).



- [11] X. Kong and F. Ravndal, Nucl. Phys., **A656**, 421 (1999); **A665**, 137 (2000); X.-w. Kong and F. Ravndal, Phys. Lett., **B470**, 1 (1999); X. Kong and F. Ravndal, **B450**, 320 (1999); Phys. Rev., **C64**, 044002 (2001).
- [12] L. H. Kawano, W. A. Fowler, R. W. Kavanagh, and R. A. Malaney, Astrophys. J., **372**, 1 (1991).
- [13] L. Trache *et al.*, Phys. Rev. C, **67**, 062801 (2003).
- [14] L. Koester, K. Knopf, and W. Waschkowski, Z. Phys., **A312**, 81 (1983); C. Angulo *et al.*, Nucl. Phys., **A716**, 211 (2003).
- [15] D. B. Kaplan, M. J. Savage, and M. B. Wise, Phys. Lett., **B424**, 390 (1998).
- [16] P. F. Bedaque and U. van Kolck, Phys. Lett., **B428**, 221 (1998); J.-W. Chen, G. Rupak, and M. J. Savage, Nucl. Phys., **A653**, 386 (1999).
- [17] S. Typel and G. Baur, Nucl. Phys., **A759**, 247 (2005).
- [18] S. Choi, J. Lee, J. S. Shim, and H. Song, J. Korean Phys. Soc., **25**, 576 (1992); S. Fleming, T. Mehen, and I. W. Stewart, Nucl. Phys., **A677**, 313 (2000).
- [19] L. S. Brown, *Quantum Field Theory* (Cambridge University Press, 1994).
- [20] F. C. Barker, Nucl. Phys., **A588**, 693 (1995).
- [21] J. C. Blackmon *et al.*, Phys. Rev. C, **54**, 383 (1996).
- [22] H. W. Hammer and D. Lee, Phys. Lett., **B681**, 500 (2009); Annals Phys., **325**, 2212 (2010).
- [23] W. L. Imhof, R. G. Johnson, F. J. Vaughn, and M. Walt, Phys. Rev., **114**, 1037 (1959), the two data sets correspond to two different normalizations of the same data.
- [24] J. E. Lynn, E. T. Jurney, and S. Raman, Phys. Rev. C, **44**, 764 (1991).
- [25] Y. Nagai *et al.*, Phys. Rev. C, **71**, 055803 (2005).
- [26] R. Higa and G. Rupak, in preparation.